NUMERICAL SIMULATION OF THE 2011 TOHOKU EARTHQUAKE TSUNAMI AND INUNDATION WITH MOHID

S.-K. Hyun • J.-Y. Choi • D.-Y. Lee • K.-H. Cho

CHAPTER SYNOPSIS

Background

From experiences on massive tsunami damages occurred in Indonesia on 25 October 2010 and Japan on 11 March 2011, we have learned that the development of a tsunami forecast system for the northwestern regions of the Pacific Ocean is required. We applied a multi-functional three-dimensional circulation model, MOHID, for the 2011 Tohoku earthquake tsunami and inundation simulations to determine if the model is appropriate to the forecast system.

Results

With three-level nested grids, we carried out tsunami and inundation simulations. In the tsunami simulation, MOHID represented reasonably the tendency of the observed tsunami with respect to tsunami height and arrival time of the maximum height. With the refined grids of 1/150º and 1/600º, the simulated inundation area and height were fairly well matched with a satellite image along the Japanese coast.

Conclusions

It is found that the increase of horizontal resolution in coastal regions up to 1/600º improved the result of coastal inundation showing the good agreement with the satellite image. Overall, it is concluded that MOHID is appropriately applied to the tsunami and inundation forecast system for the northwestern regions of the Pacific Ocean.

1 INTRODUCTION

Most of major tsunamis have been generated by undersea earthquakes. In deep water, tsunamis propagate very fast with long wavelengths and small amplitudes. A leading tsunami wave can be considered as a long wave with a propagating speed that is proportional to $(gh)^{1/2}$, where g is the gravitational constant ($m\,s^{-2}$) and h is the water depth (m). However, tsunami approaches shore where the water depth becomes shallow, the amplitude of the tsunami increases and the wavelength decreases. A tsunami can cause severe coastal flooding and property damages [1]. Historically tsunamis have rarely occurred around Korea peninsula. However, once the tsunamis happen in the East Sea, they make massive damages to the Korean, Japanese, and Russian coasts. Among the tsunamis occurred in the East Sea, the ones on 26 May 1983 and 12 July 1993 influenced the east coast of Korea. In particular, the tsunami in 1983 brought big inundation damages on Mukho and Imwon Harbors [2].

With increasing the activities of the earthquakes occurred in Chile on 27 February 2010, Indonesia on 25 October 2010, and Japan on 11 March 2011, we have learned that Korea is not a safe zone from the sea earthquakes and the corresponding tsunamis. It deserves to develop a tsunami forecasting system for the East Sea, the Yellow Sea, and the regional seas of Korea using an appropriate numerical model. Therefore, in the present study, the objectives are to investigate the propagation of the tsunami wave and inundation caused by the earthquake occurred in Japan on 11 March 2011 using a multi-functional three-dimensional

circulation model, MOHID, and to examine MOHID's applicability for the tsunami and inunda-tion simulations. MOHID will be applied for the initial surface deformation estimated by elastic finite fault plane theory which represents the instantaneous seafloor rupture [3, 4].

2 INFORMATION OF SIMULATION

2.1 2011 Japan Earthquake and Tsunami

A massive earthquake of moment magnitude (M_w) of 9.0 occurred at 05:46 (UTC) on 11 March 2011, off the eastern coast of Japan (Tohoku region). This earthquake, 'the 2011 off the Pacific coast of Tohoku Earthquake' named by the Japan Meteorological Agency [5], is the largest one recorded in Japan. The focal area estimated from the distribution of aftershocks stretches about 500 km long and 200 km wide offshore [6]. Its epicenter was approximately 70 km east of the Oshika Peninsula, its hypocenter was located about 130 km east-southeast off Oshika Peninsula, and the observed maximum slip was approximately 24 m near the hypocen-ter [7]. The earthquake triggered the devastating tsunami waves which reached heights of up to 39.7 m in Miyako in Tohoku's Iwate Prefecture and caused the maximum inundation height (19.5 m) on the Sendai Plain, and the tsunami bore propagated more than 5 km inland [8]. The amplified tsunami can be formed through topographic refraction when tsunamis travel along ocean ridges and seamount chains in the Pacific Ocean [9]. The tsunami caused the tremendous loss of ten thousand lives and an astronomical damage cost (309 billion USD). JMA reported offshore tsunami heights recorded from wave height meter buoys were 6.3 m at Miyako, 6.0 m at Kuji, and 6.0 m at Miyagi.

2.2 MOHID modelling system and measurements

The MOHID Water Modeling System [10] was applied to estimate the tsunami wave propa-gation and inundation along the north-east coast of Japan during 2011 Tohoku earthquake. A three-level nesting scheme was used for tsunami simulations (Figure 1). As described in Table 1, the numerical experiments for 2011 Japan tsunami were carried out with three different level grids in horizontal. For the tsunami simulation, a resolution of $1/30^o$ ($\sim$3.6 km) is used at the Level-1 grid which is ranging from 25.0^o to 47.0^o N in latitude and from 127.3333^o to 157.0^o E in longitude. The result of the tsunami wave propagation computed at the Level-1 grid will be compared with the tsunami data observed by NOAA National Data Buoy Center (NDBC) and UNESCO/IOC Sea Level Station Monitoring Facility.

The experiment for tsunami inundation is performed at the Level-3 grid which resolu-tion is $1/600^o$ ($\sim$180 m) in latitude and longitude because the inundation simulation requires much higher resolution to resolve the wetting and drying areas. The interfacial resolution at the Level-2 grid is $1/150^o$ ($\sim$720 m) which is 5 times finer than Level-1 and 4 times coarser than Level-3. To generate Level-1 and Level-2 grids, we utilize ETOPO-1 bathymetry dataset obtained from NOAA's National Geophysical Data Center (NGDC) and shoreline data from NOAA coastline extractor. For the Level-3 grid generation, we combined 30-arc second bathymetry data from the General Bathymetric Chart of the Oceans (GEBCO) of the British Oceanographic Data Center (BODC) with 90-m resolution digital elevation model (DEM) data

Table 1. *Information of constructed model system.*

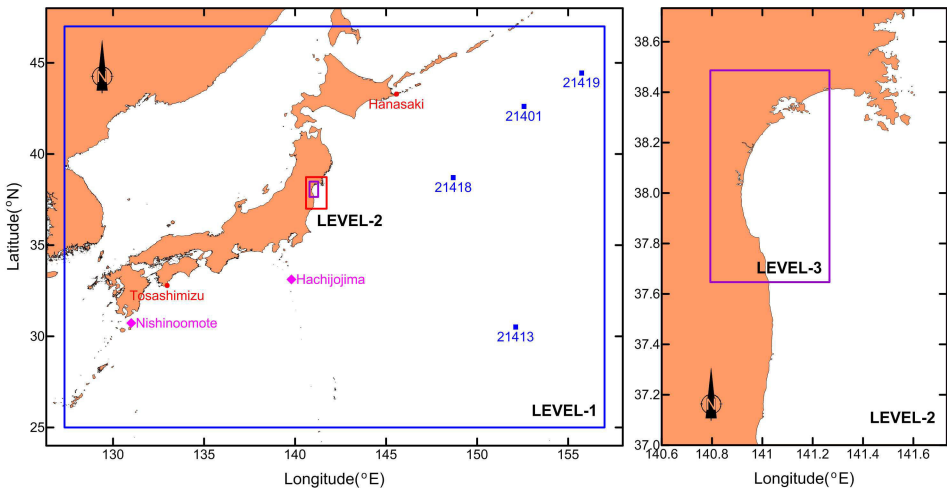| Model	Modeled Area	Resolution	Number of Grid cells		Δt(sec)
			x	y	
Level-1	25.0000~47.0000 °N 127.3333~157.0000 °E	1/30 °	890	660	10
Level-2	37.0~38.7333 °N 140.6000~141.7333 °E	1/150 °	170	260	5
Level-3	37.6467~38.4867 °N 140.7933~141.2666 °E	1/600 °	284	504	5

Figure 1. *Simulation domain with three-level nesting grid system including observation stations: DART buoy (blue squares), IOC (red circles), and JCG (pink diamonds).*

from the Shuttle Radar Topography Mission (SRTM3) operated by the U.S. Geological Survey (USGS) (Figure 2). For the tsunami simulation, we considered initial water surface displacement obtained from an elastic fault plane model as an initial condition and simulated until 5 hours after the earthquake occurred. Detailed information on MOHID can be found in [11].

2.3   Tsunami source: Initial water surface displacement

Initial water surface displacement caused by Tohoku earthquake is calculated by the elastic fault plane model [4] which is included in the Cornell Multi-grid Coupled Tsunami model version 1.7 (COMCOT) [12]. The fault model assumed that the water surface displacement is the equivalent of the seafloor deformation since the uplift motion is much faster than the wave propagation. To compute the deformation, fault parameters are necessary to be defined [12]. The definition of fault parameters is depicted in Figure 3. The detailed procedure of elastic fault plane theory can be found in the [3, 4]. In this experiment, fault parameters are determined from double fault data calculated by Geospatial Information Authority of Japan [7]

as described in Table 2. The initial epicenter is located in the position released from JMA (142.861° E, 38.104° N). It is assumed that two rectangular faults are slipped uniformly. Total fault length is approximately 380 km (northern segment: 186 km, southern segment: 194 km) and total moment magnitude is M_w 8.9 (northern segment: M_w 8.8, southern segment: M_w 8.3). Consideration of double faults is suggested to be more reasonable than that of a single fault [13]. Besides, horizontal and sectional distributions of initial water surface displacement calculated by [4] fault model are shown in Figure 4. In the AA' section, the predicted maximum and minimum water heights are approximately 11.2 m and -3.8 m, respectively.

Table 2. *Fault parameters for the 2011 Tohoku earthquake.*

	Lat. (°)	Lon. (°)	Depth (Fault Top, km)	Length (km)	Width (km)	Strike (°)	Dip (°)	Rake (°)	Slip (m)	M_w
Fault 1	38.80	144.00	5.1	186	129	203	16	101	24.7	8.8
Fault 2	37.33	142.80	17.0	194	88	203	15	83	6.1	8.3

3 RESULTS OF SIMULATION

3.1 Tsunami simulation with the first level grid

The tsunami predicted at MOHID Level-1 is compared with sea surface elevation data obtained from three resources: 1) Deep-ocean Assessment and Reporting of Tsunamis (DART) Buoys operated by NOAA National Data Buoy Center (NDBC), 2) UNESCO/IOC seal level station monitoring facility, and 3) Japan Coast Guard (JCG). Tidal signals in observation data were removed through a 3-h high-passed filter [14] to fairly compare with the predicted tsunami. At eight stations (21401, 21413, 21418, 21419, Hanasaki, Tosashimizu, Hachijo-jima, and Nishinoomote, see Figure 1), the time series comparisons between the predicted and observed tsunamis are plotted in Figure 5. The prediction has a reasonable agreement with the observation showing 10~45 cm of root-mean-squared-error. Especially, the predicted tsunamis reproduced the observed tsunamis well at offshore stations (21401, 21413, 21418, and 21419) where are less influenced by geometry and topography.

At the Hachijojima and Nishinoomote stations, the model results were reasonably well compared with the observations. However, the comparisons at Japan coastal stations (Hanasaki and Tosashimizu) represented the increase of bias between model result and observation data. This bias seems to be induced by the use of 1/30° resolution in ETOPO-1 topographic data. It seems that wave propagation and deformation induced by depth change were inaccurately computed in the grid generated with low resolution topographic data. Thus, it is expected that the usage of higher resolution bathymetry data may improve the accuracy of tsunami prediction. As shown in Figure 6, horizontal distributions of tsunami height at Level-1are plotted on 5 minutes, 10 minutes, 30 minutes, and 60 minutes after tsunami occurred. The maximum height is generated from the northern segment and spreads to the coastal areas and to the Pacific Ocean.
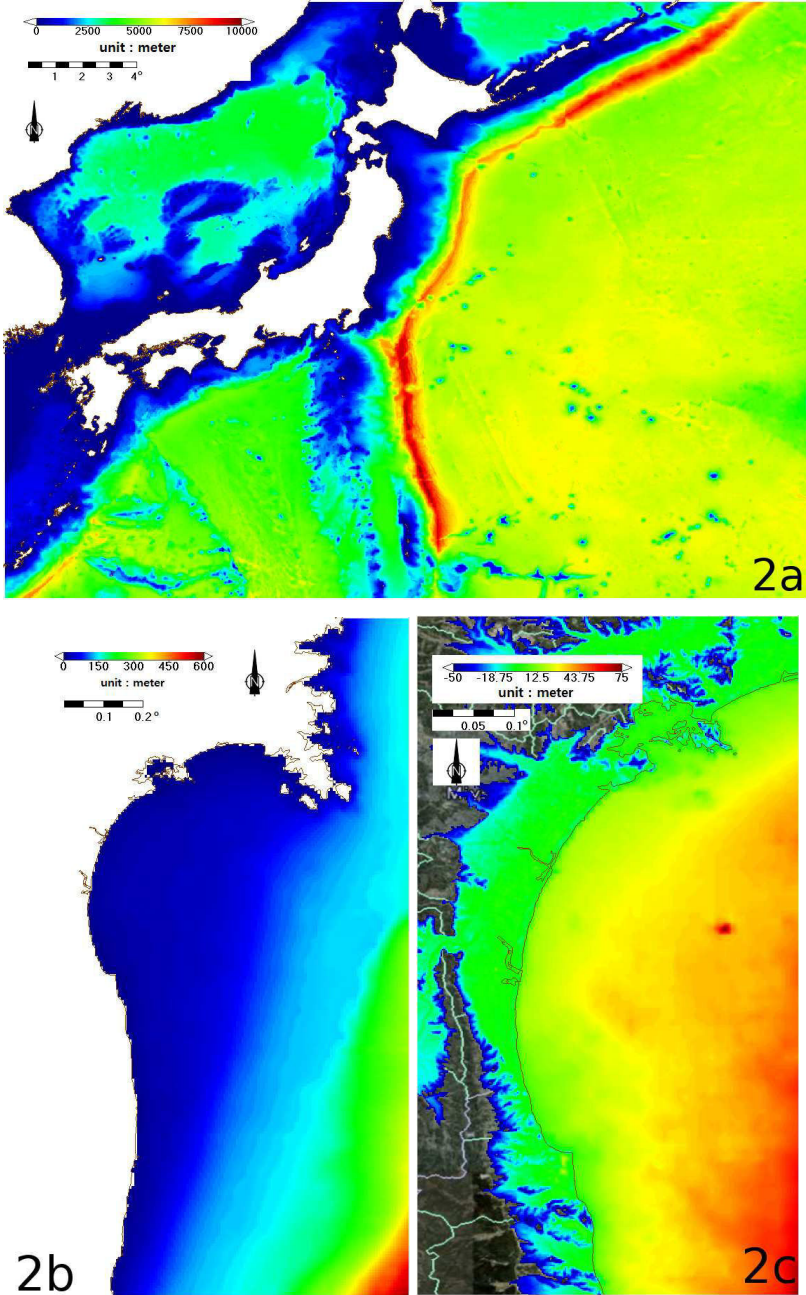
Figure 2. *Applied bathymetry and topography to the three-level nesting grid system: (a) Level-1, (b) Level-2, and (c) Level-3.*
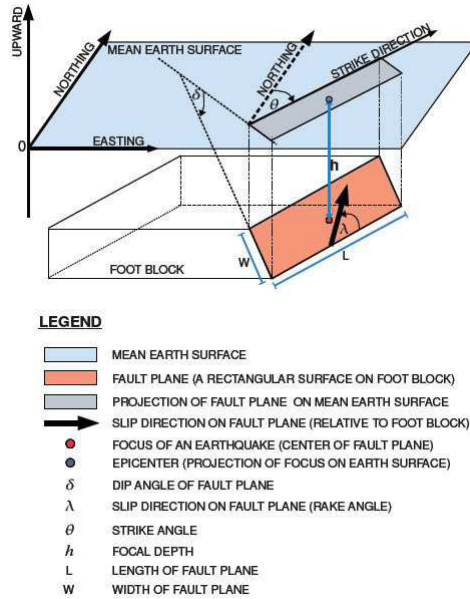
Figure 3. *Sketch of a fault plane and fault parameter definitions [12].*
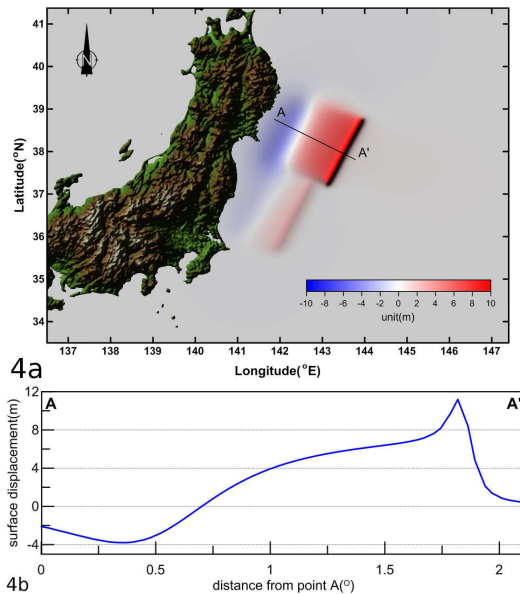

4a

4b

Figure 4. *Tsunami source estimated by a fault plane model. (a) Horizontal initial water surface displacement and (b) Surface displacement from A to A'.*
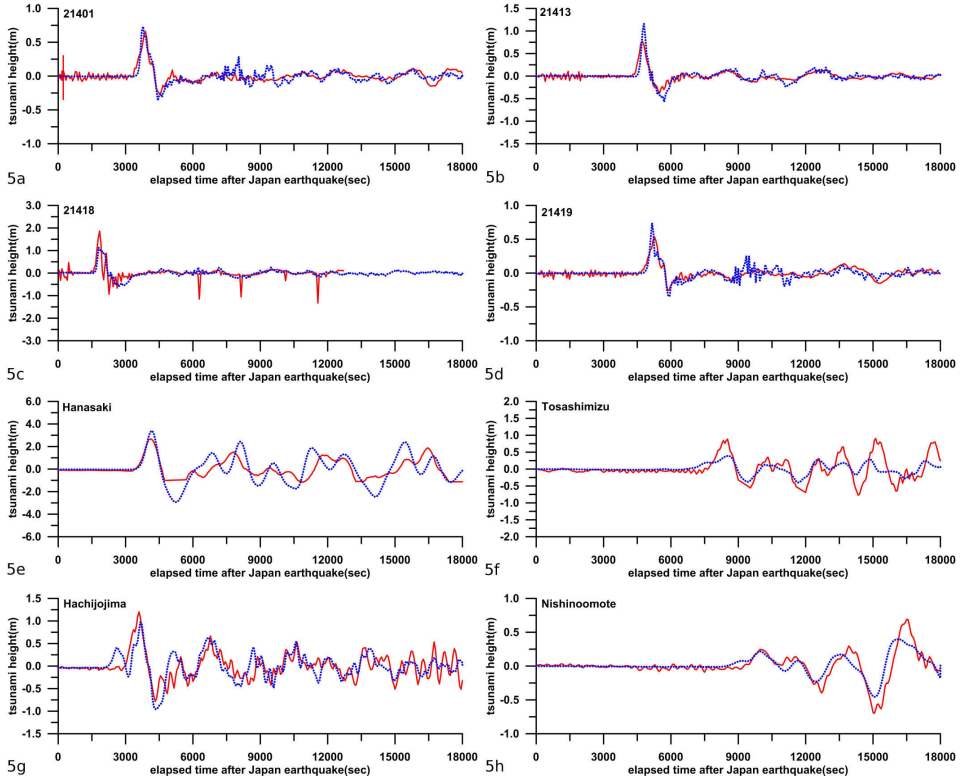
Figure 5. *Comparisons of tsunami height between the observed data (red) and computed results (blue).*

We estimated the arrival time of the first maximum tsunami peak to individual stations to evaluate the model performance. As shown in Table 3, the peak time differences between the observed and the predicted at all stations were within two minutes and it is confirmed that the corresponding tsunami wave speeds were computed reasonably well. A snapshot of the maximum tsunami height predicted at Level-1 during 5-hour simulation period is depicted in Figure 7. The maximum tsunami heights are concentrated on the northern segment of faults and the eastern coast of Japan. In the coastal region of Miyako, the highest maximum value is approximately 23.8 m which is nearly 40% less than the observation.

3.2 Inundation simulation with higher level grids

To predict the influence of inundation induced by tsunami on the Japanese coast, the second-level nesting experiments are implemented using the refined grids of 1/150 ° (Level-2) and 1/600° (Level-3). Figure 8 represents the inundation areas with tsunami height compared with the TerraSAR-X image taken by the Center for Satellite Based Crisis Information (ZKI) on 12 March 2011. We overlapped the model result onto the satellite image. The simu-lated inundation areas (purple) are fairly well matched with the TerraSAR-X inundation areas (blue) along the Japanese coast. The along-shore distribution of the inundation height in the
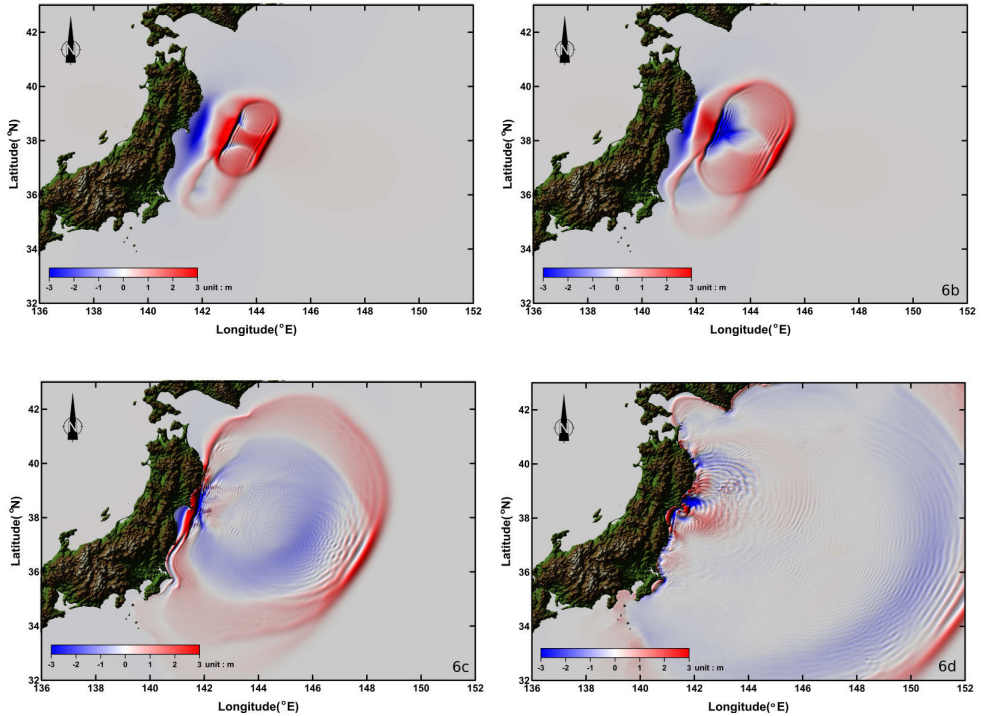
Figure 6. *Horizontal distributions of the modelled tsunami height snapshotted at (a) 5 minutes, (b) 10 minutes, (c) 30 minutes, and (d) 60 minutes after the earthquake.*

uppermost water cells is depicted in Figure 9. The inundation heights were estimated at the survey locations (Figure 9a). The survey data are obtained from The 2011 Tohoku Earthquake Tsunami Joint Survey Group [15] and available at ftp://ftp.agu.org/apend/gl/2011gl049210 [8]. The predicted inundation heights (blue in Figure 9b) were compared with the measured inundation heights (red in Figure 9b). The inundation heights around Natori, Iwanuma, Watari, and Arahama areas were fairly well matched with measurements even though those near Miyagi and Sendai areas were underestimated. It is expected that the use of much higher resolution of bathymetry and geometry data can improve the model results.

4   DISCUSSION AND SUMMARY

In the tsunami simulation for the Japan Tohoku Earthquake in 2011, the MOHID represented reasonably the tendency of the observed tsunami. In Level-1 ($1/30^o$) simulation, tsunami bias at onshore stations is larger than that at offshore stations due to the coarse grid which may not accurately resolve the bathymetry and coastline. However, the predicted arrival time of the first maximum tsunami wave is well matched with the observation record lagged within only 2 minutes. The increase of horizontal resolution in coastal regions up to $1/600^o$ (Level-3) improved the result of coastal inundation induced by tsunami waves showing the good agreement with the satellite image.
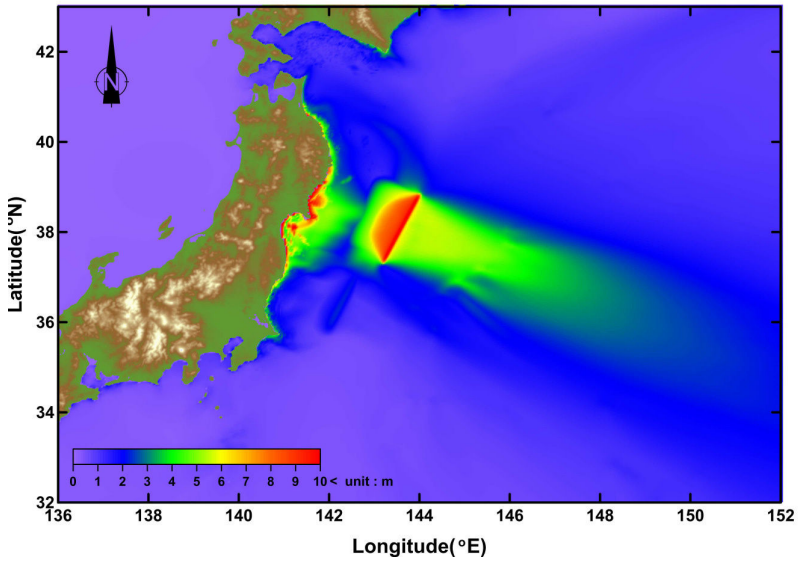
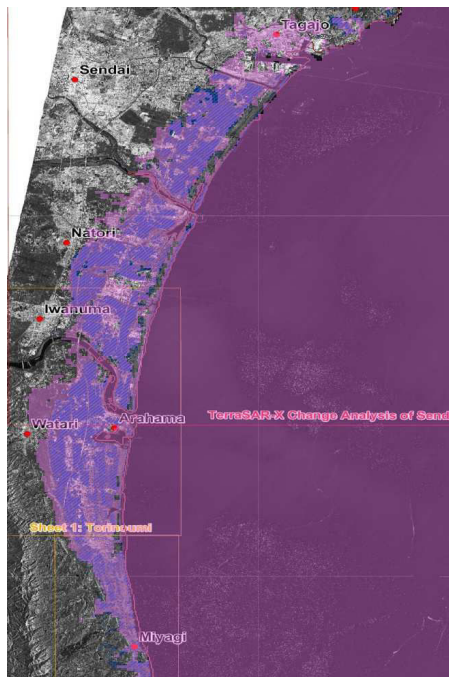**Figure 7.** *Maximum tsunami height during 5 hours computed in Level-1 simulation.*

Figure 8. *Comparison of the computed inundation area (purple) with the TerraSAR-X satellite image (blue-shaded).*
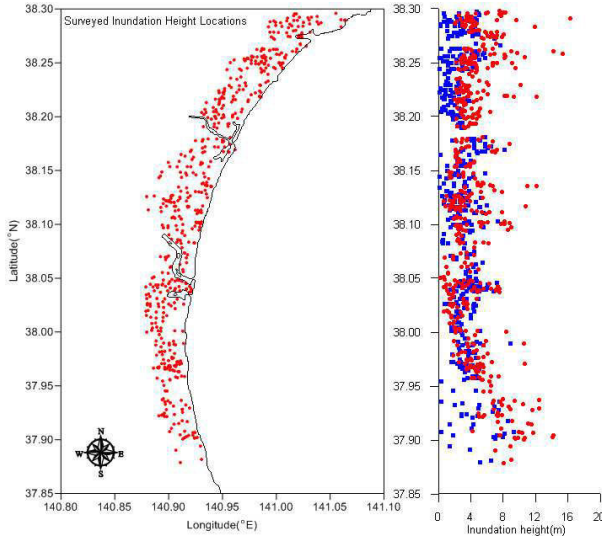
Figure 9. *Survey locations for inundation height (left) and comparison of inundation height (right) between observations (red dots) and computed results (blue squares).*

Table 3. *Arrival time of the first maximum tsunami wave heights at the stations with comparisons between observations and predictions.*

station	Arrival time in minutes	
	observed	calculated
21401	65	63
21413	79	80
21418	31	30
21419	88	86
Hanasaki	68	69
Tosashimizu	142	142
Hachijojima	60	61
Nishinoomote	166	166

A further study is required to quantitatively analyze the model skill comparing the inundation areas and inundated water volume. The inundation height comparison with observation suggests that a higher resolution grid model with more accurate coastal bathymetry and topography data improves the tsunami height and inundation prediction. It is notable that a model grid which does not resolve the barriers and structures to protect tsunami waves is insufficient to predict inundation height and run-up height on the local areas, because sea walls, barriers, structures, and debris may play important roles in changing local tsunami propagation. Furthermore, the tsunami and inundation prediction needs to be combined with the external forcing such as tides, currents, and winds in a real-time oceanic forecast system to warn the tsunami coming immediately.

REFERENCES

1. Liu, P. L.-F., S.-B. Woo, and Y.-S. Cho, 1998. Computer programs for tsunami propagation and inundation, Cornell University.

2. Choi, B.-H., S.-J. Hong, S.-B. Woo, and E. Pelinovsky, 2000. Computation of Tsunamis in the East Sea using Dynamically Interfaced Nested Model. Korean Society of Coastal and Ocean Engineers, 11, pp. 47-54.

3. Mansinha, L. and D. E. Smylie, 1971. The displacement fields of inclined faults. Bulletin of Seismological Society of America, 61, pp. 1433-1440.

4. Okada, Y., 1985. Surface deformation due to shear and tensile faults in a half-space. Bulletin of Seismological Society of America, 75, pp. 1135-1154.

5. Japan Meteorological Agency (JMA), 2011: `www.jma.go.jp/jma/en/2011_Earthquake.html`.

6. Sato, M., T. Ishikawa, N. Ujihara, S. Yoshida, M. Fujita, M. Mochizuki, and A. Asada, 2011. Displacement above the hypocenter of the 2011 Tohoku-Oki Earthquake. Science, 332, 1395

7. Geospatial Information Authority of Japan (GSI), 2011: `www.gsi.go.jp/cais/topic110422-index-e.html`.

8. Mori, N., T. Takahashi, T. Yasuda, and H. Yanagisawa, 2011. Survey of 2011 Tohoku earthquake tsunami inundation and run-up. Geophysical Research Letters, 38, L00G14, doi:10.1029/2011GL049210.

9. Song, Y.T, I. Fukumori, C.K. Shum, and Y. Yi, 2012. Merging tsunamis of the 2011 Tohoku-Oki earthquake detected over the open ocean. Geophysical Research Letters, 39, L05606, doi:10.1029/2011GL050767.

10. Cancino L, Neves R. 1999. Hydrodynamic and sediment suspension modelling in estuarine systems. Part I: Description of the numerical models. Journal of Marine Systems, 22, pp. 105-116.

11. Ribeiro, J., A. Silva, and P. Leitão, 2011. High resolution tsunami modelling for the evaluation of potential risk areas in Setúbal (Portugal). Natural Hazards and Earth System Science, 11, pp. 2371-2380.

12. Wang, X., 2009. User manual for COMCOT version 1.7. Cornell University.

13. Bae, J.S., Y.J. Cho, S.J. Kwon, and S.B. Yoon, 2012. Numerical analyses of 2011 East Japan tsunami propagation towards Korean peninsula. Journal of Korean Society of Coastal and Ocean Engineers, 24, pp. 66-76 (In Korean).

14. Rabiner, L. and B. Gold, 1975. Theory and application of digital signal processing. Prentice-Hall, Englewood Cliffs, New Jersey.

15. The 2011 Tohoku Earthquake Tsunami Joint Survey Group, 2011. Nationwide field survey of the 2011 off the Pacific coast of Tohoku earthquake tsunami, Journal of Japan Society of Civil Engineers, 67, pp. 63-66.